

# Neutrino mean free path in neutron stars

Caiwan Shen<sup>1,2</sup>, U. Lombardo<sup>1,3</sup>, N. Van Giai<sup>4</sup>, and W. Zuo<sup>5</sup>

<sup>1</sup>*INFN-LNS, Via Santa Sofia 44, I-95123 Catania, Italy*

<sup>2</sup>*China Institute of Atomic Energy, P.O.Box 275(18), Beijing 102413, China*

<sup>3</sup>*Dipartimento di Fisica, Via Santa Sofia 64, I-95123 Catania, Italy*

<sup>4</sup>*Institut de Physique Nucléaire, F-91406 Orsay, France*

<sup>5</sup>*Institute of Modern Physics, Chinese Academy of Sciences, Lanzhou, China*

The neutrino propagation in neutron stars is studied in the framework of the linear response method. The medium effects are treated in the non-relativistic Brueckner-Hartree-Fock approach either in the mean-field approximation or in the RPA. The residual interaction is expressed in terms of the Landau parameters extracted from the equation of state of spin- and isospin-polarized nuclear matter. The Brueckner theory including three-body forces is used for determining the equation of state. Numerical predictions for the response function of nuclear matter in  $\beta$ -equilibrium and the neutrino mean free path are presented in a range of baryonic densities and temperatures. The main results are a dominance of the charge-exchange component over the scattering component and an enhancement of the neutrino mean free path induced by nuclear correlations.

PACS numbers: 26.60.+c, 26.50.+x

## I. INTRODUCTION

The interaction of neutrinos with baryons has been mostly studied in connection with the stability of nuclei, but it also plays a crucial role in the thermal evolution of supernovae and protoneutron stars, where the nuclear medium exhibits quite distinctive physical features related to density, temperature and chemical composition. A large effort has been devoted to study the production of neutrinos via direct or modified URCA processes [1] and, more recently, via the bremsstrahlung of nucleons in the strong magnetic field of neutron stars [2]. In the past simulation codes have incorporated the propagation of neutrinos in neutron matter mostly by using the Fermi-gas model, whereas the effects of correlations did not receive the due consideration except in a few cases [3, 4, 5]. In the recent years calculations of correlation effects have been performed, including phenomenological approaches with Skyrme forces [6, 7, 8], microscopic Brueckner theory [4, 5, 9, 10] and relativistic mean field theory [11, 12, 13, 14, 15, 16, 17, 18]. On the other hand, in order to reliably describe the correlations of nuclear matter in extreme conditions, one needs a well developed microscopic many-body theory, since not enough experimental constraints exist so far in a so wide range of density, temperature and isospin asymmetry which are supposed to occur in the present neutron-star models.

In this paper we present a study of the nuclear response function to weak interaction and the effects of short- and long-range correlations on the neutrino transport in neutron stars. It is based on the equation of state (EOS) predicted by the Brueckner theory approach including relativistic effects and nucleonic resonances. Recently this approach has made a step forward in reproducing the empirical saturation properties of nuclear matter [19, 20]. The particle-hole NN residual interaction is extracted from the Brueckner theory and cast in terms of the Landau parameters. The response function to the

neutrino propagation is calculated first in the Brueckner-Hartree-Fock (BHF) limit, and then in the random phase approximation (RPA) in neutron matter in  $\beta$ -equilibrium with protons and electrons for various conditions of neutron density and temperature. The neutrino mean free path (MFP) is also calculated taking into account the  $(\nu_e, \nu'_e)$  scattering from nucleons and the  $(\nu_e, e^-)$  charge-exchange process. In this work we discuss only the  $\nu_e$  case which is the most important one for the MFP issue.

## II. NUCLEAR MATTER IN THE BHF APPROXIMATION

A neutron star, in the most simplified model, is made of neutrons, protons and electrons, and the relative abundance is controlled by the  $\beta$ -equilibrium condition (the effect of muons is negligible). Under the condition of charge neutrality, the proton fraction  $Y_p = Z/A$  is driven by the value of the symmetry energy at a given total baryonic density. Here, we will always consider nuclear matter in  $\beta$ -equilibrium unless explicitly stated.

Our framework is the Brueckner-Bethe-Goldstone (BBG) approach, where the perturbative expansion of the total energy per particle  $E_A$  can be cast according to the number of hole lines. The lowest order defines the Brueckner-Hartree-Fock approximation, which exhibits a satisfactory convergence provided the continuous choice for the mean field is adopted [21].

In the recent years a remarkable step forward in the reproduction of the empirical saturation properties has been performed including three-body forces (3BF) in the BBG theory [19, 20]. Their effect in fact is twofold: on one hand, it brings the saturation density of nuclear matter close to the empirical value; on the other hand, it provides the high-density strong repulsive components. As a consequence the BHF approximation has reached the level of a consistent description of a strongly correlated

Fermi system in the region of saturation density as well as in high density regions.

A microscopic derivation of the full set of  $l = 0$  Landau parameters can be done, based on the BHF approximation, from the calculation of the energy per particle of nuclear matter in different states of spin and isospin polarization. Starting from unpolarized symmetric nuclear matter at a given density  $\rho$ , we may extend the calculation of  $E_A$  to isospin density variations  $\delta\rho_\tau = (\rho_\tau - \rho)/\rho$  and spin-isospin density variations  $\delta\sigma_\tau = (\rho_\tau^\uparrow - \rho_\tau^\downarrow)/\rho_\tau$ . The response of the system is related to the second derivatives of the expansion of  $E_A$ ,

$$E_A(\rho, \delta\rho_n, \delta\rho_p) = E_A(\rho) + \frac{1}{2} \sum_{\tau\tau'} \Phi_{\tau,\tau'} \delta\rho_\tau \delta\rho_{\tau'}, \quad (1)$$

$$E_A(\rho, \delta\sigma_n, \delta\sigma_p) = E_A(\rho) + \frac{1}{2} \sum_{\tau\tau'} \Gamma_{\tau,\tau'} \delta\sigma_\tau \delta\sigma_{\tau'}. \quad (2)$$

These derivatives give the  $l = 0$  Landau parameters of the residual NN interaction,

$$F_0 = F_{nn}^0 + F_{np}^0 = \frac{4N(0)}{\rho} (\Phi_{nn} + \Phi_{np}) - 1, \quad (3)$$

$$F'_0 = F_{nn}^0 - F_{np}^0 = \frac{4N(0)}{\rho} (\Phi_{nn} - \Phi_{np}) - 1, \quad (4)$$

$$G_0 = G_{nn}^0 + G_{np}^0 = \frac{4N(0)}{\rho} (\Gamma_{nn} + \Gamma_{np}) - 1, \quad (5)$$

$$G'_0 = G_{nn}^0 - G_{np}^0 = \frac{4N(0)}{\rho} (\Gamma_{nn} - \Gamma_{np}) - 1, \quad (6)$$

where  $N(0)$  is the level density at the Fermi surface. Notice that our definitions Eqs.(3)-(6) differ by a factor of 2 from that of other authors, for instance [23]. The Landau parameters are constrained by robust physical observables.  $F_0$  is in fact constrained by the compression modulus, whose value should range in the interval 230-250 MeV according to the experimental determination of the monopole giant resonance energy centroid.  $F'_0$  is related to the symmetry energy, which at the saturation density is reported about 30 MeV in the Bethe-Weizsacker mass formula.  $G_0$  is related to the spin modes, which actually are hardly observed in nuclei. So far experimental information on  $G_0$  is not enough since spin resonances have only been observed with too small strength compared to other collective modes[22]. Finally  $G'_0$  is constrained by the Gamow-Teller giant resonance. A value of 1.2 at the saturation point has been determined with high precision from the experimental excitation energy of the Gamow-Teller resonance on  $^{90}\text{Ni}$  [23]. The BHF prediction of the Landau parameters is reported in Fig.1. They have been obtained from a BHF calculation with the Argonne  $AV_{18}$  [24] as two-body force (2BF) and a microscopic three-body force which corrects the BHF approximation by relativistic effects and nucleonic virtual excitations[25].

The prediction of the Landau parameters for densities other than the nuclear density is of great interest in the study of neutron stars. In connection with the strong

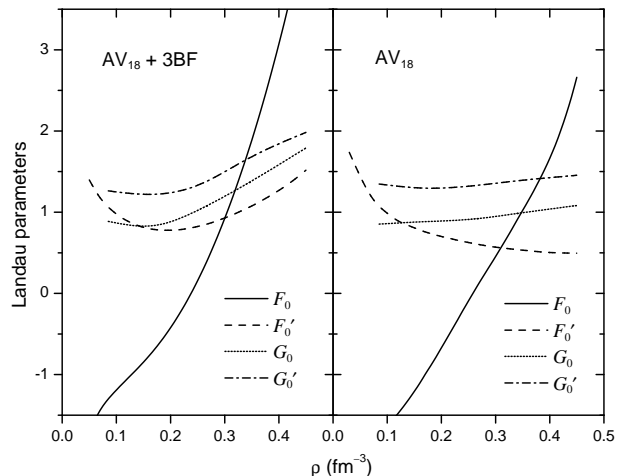


FIG. 1: Landau parameters of symmetric nuclear matter with 2BF  $AV_{18}$  (right) and the same plus 3BF (left)

magnetic fields observed in neutron stars some authors have studied the magnetic susceptibility in neutron matter and found that  $G_0$  reduces the susceptibility of the degenerate neutron gas[26, 27, 28, 29]. This reduction is amplified at high density when including 3BF either in Brueckner calculations[28] or in Monte Carlo many-body simulations [26].

In this work it is assumed that the Landau parameters do not change appreciably with temperature, which is certainly a good approximation below the liquid-to-gas phase transition ( $T_c \approx 18\text{MeV}$ ). This point will be discussed in more details in section IV(A).

### III. INTERACTION OF NEUTRINOS WITH MATTER

During their propagation in neutron-star matter neutrinos experience collisions with nucleons via weak coupling with the nucleon neutral currents  $j_\mu = \bar{\psi}_\tau \gamma_\mu (c_v^\tau - c_a^\tau \gamma_5) \psi_\tau$ . Neutrinos can also disappear in the charge-exchange process  $\nu_e + n \rightarrow e^- + p$  and we also consider the coupling with charged currents  $j_\mu = \bar{\psi}_p \gamma_\mu (g_v - g_a \gamma_5) \psi_n$  giving rise to neutrino absorption. The vector and axial coupling constants for neutral currents are  $c_v^\tau$  and  $c_a^\tau$ , and for charged currents  $g_v$  and  $g_a$  (a complete list of the constants is given in Ref.[7]).

The neutrino MFP  $\lambda$  is derived from the transport equation

$$\frac{c}{\lambda_{\vec{k}}} = \sum_{\vec{k}'} W_{fi}(k - k')(1 - n_{\vec{k}'}) + W_{fi}(k' - k)n_{\vec{k}'}, \quad (7)$$

where  $n_{\vec{k}}$  is the occupation number of neutrinos and  $W_{fi}$  is the transition probability corresponding to the individual processes under consideration.

In the non-relativistic limit the transition rate can be

written[3, 4, 5]

$$W_{fi} = G_w^2 [(1 + \cos \theta)W_v + (3 - \cos \theta)W_a], \quad (8)$$

where  $G_w$  is the weak coupling constant,  $\theta$  is the scattering angle and  $W_v$  ( $W_a$ ) is the vector (axial) term. The transition rates are expressed in terms of the nuclear structure functions  $S_{v,a}^{\tau\tau'}$ . In the case of nucleon scattering the relation is

$$W_{v,a} = \sum_{\tau,\tau'} c_{v,a}^{\tau} c_{v,a}^{\tau'} S_{v,a}^{\tau\tau'}, \quad (9)$$

$$S_{v,a}^{\tau\tau'} = -\frac{1}{\pi} \frac{1}{1 - e^{q_0/kT}} \text{Im} \chi_{\tau,\tau'}^{v,a} \quad (10)$$

For the charge-exchange process the relation is

$$W_{v,a} = g_{v,a}^2 S_{v,a}^{pn}, \quad (11)$$

$$S_{v,a}^{\tau\tau'} = -\frac{1}{\pi} \frac{1}{1 - e^{(q_0 + \delta\mu)/kT}} \text{Im} \chi_{p,n}^{v,a}. \quad (12)$$

The quantity  $q_0$  is the energy transfer and  $\delta\mu$  is the shift between the neutron and proton chemical potentials. From the previous equations we see that the structure functions are, in turn, related to the response functions  $\chi$  which will be discussed in the next section.

#### IV. NUCLEAR RESPONSE FUNCTIONS

The major part of the work needed to obtain the neutrino MFP is in the calculation of the structure functions. These calculations can be performed at different levels of approximation beyond the free Fermi gas model. We will consider first the BHF approximation, which already takes into account the strong short-range correlations via the mass renormalization and the depletion of the Fermi surface; second, the particle-hole interaction will be taken into account in the RPA approximation. Since the ring diagram summation is almost a prohibitive task with the Brueckner G-matrix, we may approximate, in the low-frequency limit  $\omega/(kv_F) \ll 1$ , the G-matrix residual interaction by a Landau-Migdal form whose parameters are extracted from the BHF theory as described in the previous section.

##### A. BHF response function

In the BBG approach the expansion of the self-energy  $\Sigma_{\tau}(p, \omega)$  can also be cast as a hole line expansion, but the lowest order in the self-energy expansion does not correspond to the lowest order in the expansion of the energy per particle. According to the Landau definition of the quasiparticle energy, the BHF approximation for the self-energy should include the expansion up to the second order, the latter being the so called rearrangement term [30]. Doing so, the Hugenholtz-Van Hove theorem is

fulfilled. Once the approximation for  $\Sigma$  has been settled, the single-particle propagator takes the form

$$G_{\tau}^{-1}(p, \omega) = \omega - \frac{p^2}{2m} - \Sigma_{\tau}(p, \omega) + e_F^{\tau} \approx \frac{1}{Z_p^{\tau}} (\omega - \epsilon_p^{\tau}), \quad (13)$$

where  $\epsilon_p^{\tau}$  is the single-particle energy

$$\epsilon_p^{\tau} = \frac{p^2}{2m} + \Sigma(\epsilon_p) - e_F^{\tau} \quad (14)$$

and  $e_F^{\tau}$  is the Fermi energy. The factor  $Z_p^{\tau} = (1 - \frac{\partial \Sigma^{\tau}}{\partial \omega})_{\omega=\epsilon_p}^{-1}$  is the quasiparticle strength associated to the depletion of the occupation probability of the single-particle level  $\epsilon_p$ . In the present study the rearrangement term will be neglected, which is not a too severe approximation since it does not affect the EOS at zero temperature and, consequently, the calculation of the Landau parameters. At finite temperature it cannot be absolutely neglected, since the single-particle spectrum determines the thermal Fermi functions and hence the EOS itself.

The neutrino propagation is studied in the framework of the linear response theory. Let us first discuss the BHF limit where there are no correlations coming from the residual interaction. The dynamical structure functions are related to the imaginary part of the retarded polarization or response function  $\chi_{\tau,\tau'}^{(0)}(\vec{q}, q_0) = (\text{Re} + i \text{sign}(q_0) \text{Im}) \Pi_{\tau,\tau'}^{(0)}(\vec{q}, q_0)$ ,  $\Pi^{(0)}$  being the polarization function

$$\Pi_{\tau,\tau'}^{(0)}(\vec{q}, q_0) = -2i \int \frac{d\omega'}{2\pi} \frac{d^3 q'}{(2\pi)^3} G_{\tau}(\omega', \vec{q}') G_{\tau'}(q_0 + \omega', \vec{q} + \vec{q}'), \quad (15)$$

where the propagators are calculated according to Eqs.(13-14). One easily finds

$$\chi_{\tau,\tau'}^{(0)}(\vec{q}, q_0) = - \int \frac{d^3 p}{(2\pi)^3} Z_p^{\tau} Z_{|\vec{p}+\vec{q}|}^{\tau'} \frac{n_p^{\tau} - n_{|\vec{p}+\vec{q}|}^{\tau'}}{q_0 - \epsilon_p^{\tau} - \epsilon_{|\vec{p}+\vec{q}|}^{\tau'} + i\eta}. \quad (16)$$

According to the previous discussion the thermal occupation numbers

$$n_p^{\tau} = \frac{1}{1 + e^{(\epsilon_p^{\tau} - \epsilon_F^{\tau})/k_B T}} \quad (17)$$

are calculated from the single-particle spectrum frozen at  $T = 0$ .

##### B. RPA response function

In this subsection we study the effect of the residual particle-hole interaction. As already anticipated, the residual interaction will be described in terms of the  $l = 0$  Landau parameters discussed earlier. This makes it easier to calculate the response function  $\chi^{(\text{RPA})}(\vec{q}, q_0)$  in the RPA limit.

Let us consider first the nucleon scattering. In this case the RPA response function is given by the Bethe-Salpeter equation in the  $2 \times 2$  isospin space

$$\chi_S = \chi^{(0)} + \chi^{(0)} L^{(S)} \chi_S, \quad (18)$$

where only the diagonal elements  $\chi_{\tau,\tau}^{(0)}$  come into play and  $L_{\tau,\tau'}^{(0)} \equiv F_{\tau,\tau'}^0$  and  $L_{\tau,\tau'}^{(1)} \equiv G_{\tau,\tau'}^0$  are the matrix elements of the particle-hole residual interaction expressed by the Landau parameters (see Eqs.(3)-(6)). The  $S = 0$  ( $S = 1$ ) component is the vector (axial) part of the response function.

In the case of charge-exchange processes the Bethe-Salpeter equation is a one-dimensional equation

$$\chi_S = \chi_{p,n}^{(0)} + \chi_{p,n}^{(0)} M^{(S)} \chi_S, \quad (19)$$

where  $M^{(0)} \equiv F'_0$ ,  $M^{(1)} \equiv G'_0$ , and  $\chi_{pn}^{(0)}$  is the off-diagonal matrix element of the BHF response function.

The structure functions are essentially given by the imaginary part of the response functions, according to Eqs.(10) and (12).

## V. RESULTS AND DISCUSSION

The input data, namely the BHF mean field for the  $\chi^{(0)}$  response functions and the Landau parameters for the RPA response functions, are obtained from a non-relativistic BHF calculation of nuclear matter with the two-body  $AV_{18}$ [24] and the microscopic 3BF [25]. The temperature is set to zero, which is actually a good approximation only below the critical point, as already mentioned. The proton fraction is calculated from the symmetry energy extracted in the calculation of isospin-asymmetric nuclear matter. For  $\rho = 0.34 \text{ fm}^{-3}$ ,  $Y_p = 0.077$  without the 3BF and  $Y_p = 0.167$  with the 3BF. Thus, the 3BF has a sizable effect on  $Y_p$ .

The unperturbed (BHF) response function, as described by Eq.(16), is plotted in Fig. 2 for different temperatures and different processes. As it can be seen in the left panels (imaginary parts), the  $|\chi^{(0)}(nn^{-1})|$  is always greater than  $|\chi^{(0)}(pp^{-1})|$ . This effect, which arises from the small proton fraction, i.e., large asymmetry parameter

$$\beta \equiv \frac{N - Z}{A}$$

in neutron stars and smaller  $Z_k^p$  compared to  $Z_k^n$  from BHF calculations, gives larger scattering probability for  $\nu + n \rightarrow \nu + n$  and, consequently, shorter neutrino MFP. The response function related to scattering contributes to the neutrino MFP essentially for  $q_0 \geq 0$  whereas the one related to absorption contributes for  $q_0 \geq (\mu_p - \mu_n)$ . It also shows that the response function only depends softly on the temperature, at least in the  $T = 0$  Brueckner approximation, since the temperature appears only through  $n_k^{\tau}$ .

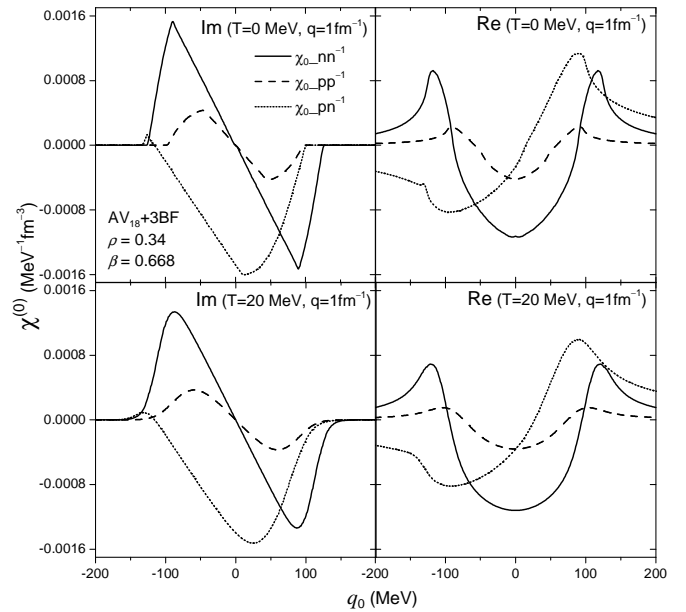


FIG. 2: The uncorrelated response functions for  $(\nu, \nu')$  scattering on neutrons ( $nn^{-1}$ , solid), on protons ( $pp^{-1}$ , dash) and neutrino absorption ( $pn^{-1}$ , dot). The imaginary part (left panel) and the real part (right panel) are plotted as functions of energy transfer. The  $\rho$ ,  $\beta$  and momentum transfer  $q$  are fixed at  $0.34 \text{ fm}^{-3}$ ,  $0.668$ ,  $1.0 \text{ fm}^{-1}$ , respectively. The upper and lower panels correspond to  $T=0$  and  $T=20 \text{ MeV}$ .

Fig.3 shows the imaginary part of the RPA response function as calculated from the Landau parameters with 3BF included. Here, we show the vector (left side) and axial (right side) components for the three isospin channels in consideration. The comparison emphasizes the dominance in both  $S = 0$  and  $S = 1$  channels of the absorption component (see insets). This effect is due to the  $q_0$  threshold (compare Eq.(10) and Eq.(12)) associated with the charge-exchange process as already discussed above.

The resonant structure of all curves is due to the collective excitations of the medium: zero sound in the case of the vector component and spin waves in protons and neutrons in the case of the axial component.

With the above response functions the neutrino MFP can be evaluated. The calculated MFP are shown as functions of the density in Fig.4 for neutral current process on the left side and charged current process on the right side.  $T$  and  $E_\nu$  are fixed to  $20 \text{ MeV}$  and  $40 \text{ MeV}$ , respectively, and  $\beta$  is fixed according to  $\beta$ -equilibrium for each density and different approximations. In order to see the different effects from the scattering process and absorption process, we divide the neutrino MFP into two parts:  $\lambda_{\text{scatt.}}$  for scattering process (left panel) and  $\lambda_{\text{absorp.}}$  for neutrino absorption process (right panel). Then, the final neutrino MFP is  $\lambda = (\lambda_{\text{scatt.}}^{-1} + \lambda_{\text{absorp.}}^{-1})^{-1}$ . Comparing the left and right panels, we get the first message that the neutrino MFP caused by the neutrino ab-

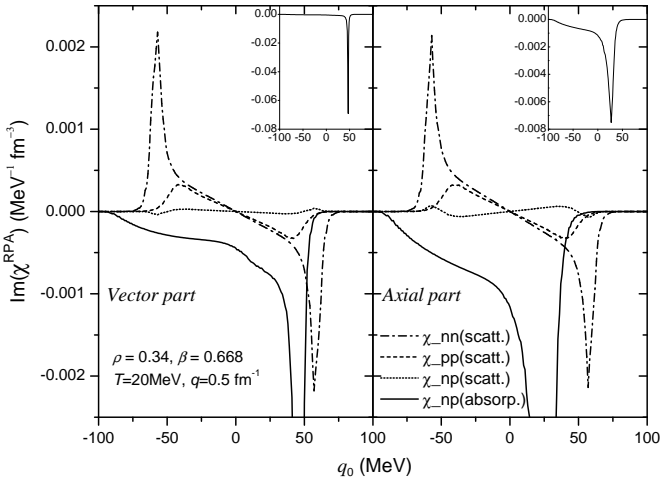


FIG. 3: Imaginary parts of RPA response functions. The vector components (left panel) and the axial-vector components (right panel) are plotted as a function of energy transfer for fixed nucleonic density, temperature and momentum transfer.

sorption is much smaller than that caused by neutrino scattering. This is a well-known effect which is due to two reasons, as noticed by Reddy et al.[6]. First, the absorption transition probability is four times the scattering transition probability; second, the absorption rate is controlled by the electron chemical potential while the scattering is controlled by the neutrino chemical potential. The inclusion of RPA correlations in the structure functions has the effect of reducing the phase space available for scattering and the MFP turns out to be substantially increased compared to the free Fermi-gas model and also to the BHF model, the latter only at high density. According to Ref.[20], the proton fraction in neutron stars increases dramatically at higher densities when the 3BF is included. This affects the behavior of the neutrino MFP in both scattering and absorption processes: the neutrino MFP increases with increasing density, especially for the neutrino absorption process. This is related to the fact that with decreasing  $\beta$ , the proton Fermi energy increases and then the reaction  $\nu_e + n \rightarrow e^- + p$  has a smaller cross section.

Since the temperature in the medium drops out rapidly in the protoneutron star, it is interesting to show the relation between neutrino MFP and temperature. In Fig. 5 (left) we plot the neutrino MFP as a function of temperature with  $\rho$ ,  $\beta$  and  $E_\nu$  fixed at  $0.34 \text{ fm}^{-3}$ ,  $0.668$  and  $40 \text{ MeV}$ , respectively. One can see the different behaviour of the scattering and absorption MFP when  $T$  increases. For the scattering process,  $\lambda$  decreases by a factor 30 from  $T=5 \text{ MeV}$  to  $T = 60 \text{ MeV}$  while for the neutrino absorption process this factor is only 2.5. In the right side of Fig. 5 the  $E_\nu$  dependence is also depicted. We just notice that the ratio between scattering and absorption MFP is almost constant.

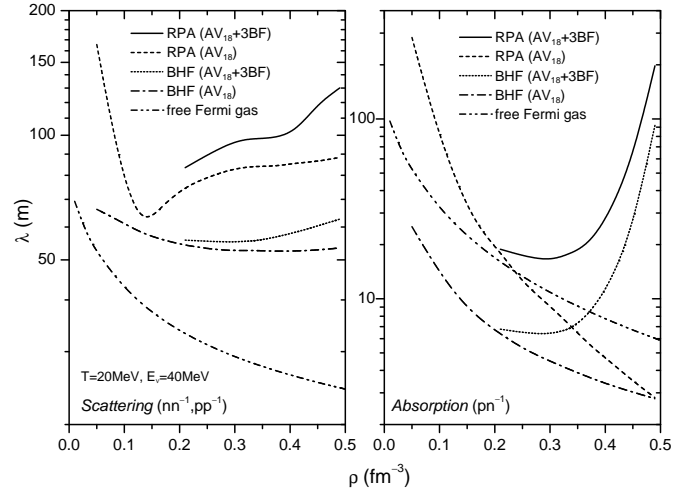


FIG. 4: Neutrino MFP for scattering (left panel) and absorption (right panel). Solid (dashed) lines: RPA with (without) 3BF; dotted (dash-dotted) lines: BHF with (without) 3BF; dash-dot-dotted lines: free Fermi-gas model. The temperature  $T$  and neutrino energy  $E_\nu$  are fixed to  $20 \text{ MeV}$  and  $40 \text{ MeV}$ , respectively.

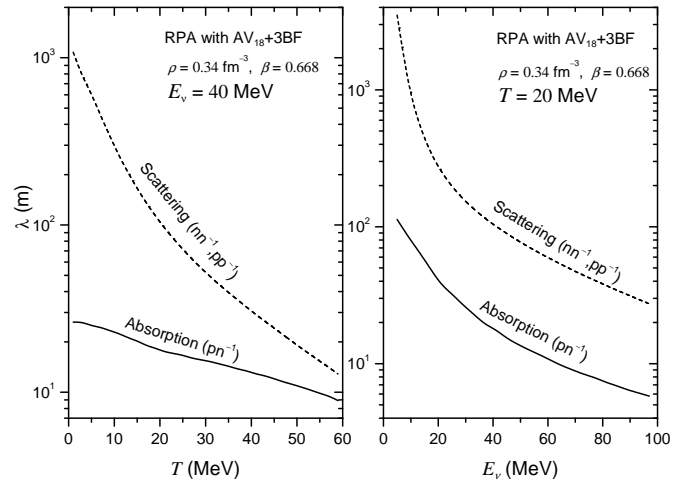


FIG. 5: Neutrino MFP vs. temperature (left) and vs. neutrino energy (right). The solid line is for neutrino absorption and dashed line for neutrino scattering. The values of  $\rho$ ,  $\beta$ , are  $0.34 \text{ fm}^{-3}$ ,  $0.668$ , respectively.

## VI. COMPARISON WITH OTHER APPROACHES AND CONCLUSIONS

The nuclear response function and the neutrino MFP in  $\beta$ -equilibrium nuclear matter have been calculated on the one hand in the BHF mean field approximation, and on the other hand in the RPA using a Landau-Migdal residual interaction to evaluate the effects of long-range correlations. Mean fields and residual interaction have been obtained within the non-relativistic Brueckner-

Hartree-Fock theory. The two-body NN potential has been supplemented by a microscopic three-body potential, which takes into account relativistic effects and also nucleonic excitations. From the present calculations one may conclude that the reduction of the neutrino MFP in the limit of the BHF mean field is much less pronounced than in the Fermi-gas model when going from low to high density. This reveals the important role of the short-range correlations incorporated in the BHF nucleon propagators. In addition, the effects of the residual particle-hole interaction have also a deep influence on the neutrino transport in  $\beta$ -equilibrium nuclear matter, resulting in a sizeable enhancement of the neutrino MFP. This result confirms the conclusion of a previous calculation of neutrino MFP in pure neutron matter [9]. At high density this effect is magnified in the absorption channel by the intense repulsive three-body force.

Since the interaction is poorly known at densities of interest in neutron star physics, the comparison with other approaches is difficult and leads often to contradictory predictions. Among the non-relativistic calculations we should quote the pioneering results by Burrows and Sawyer[4, 5]. In spite of using a different set of Landau parameters (in particular  $G_0 = 0$ ) the main features of neutrino MFP they predict are in good agreement with ours. In particular, they find an increase of  $\lambda_\nu$  by up to one order of magnitude with increasing density as an overall effect of medium correlations, and a similar temperature dependence. In the recent work of Margueron et al.[10] the emphasis is put on temperature effects in a calculation of MFP based on BHF and RPA but the 3BF is not treated and the important contribution to

the MFP due to neutrino absorption is not calculated. It is also found that the scattering MFP including RPA correlations does increase with density, similarly to our present results.

Non relativistic phenomenological approaches [6, 7, 8] manifest an opposite trend: the RPA neutrino MFP is quenched by the density increase. In fact, the residual interaction in the spin channel instead of slowly increasing at high density, decreases and finally becomes attractive. This explains also the prediction of a ferromagnetic transition in phenomenological approaches.

Relativistic approaches lead to an enhancement of the neutrino MFP when including the interaction effects in RPA even if some disagreement still exists among different calculations. In one case [13] the reduction of the scattering rate is estimated about 10% to 15%, in others [6, 12] the effect is much stronger.

A general conclusion is that the neutrino MFP is very sensitive to the EOS of nuclear matter in all aspects and it must be calculated as much as possible consistently with the EOS. In this respect we should mention a serious drawback of most calculations, which is the temperature dependence of the effective interaction. A typical value of temperature of about 20 MeV maybe is large for neglecting the effects of thermal excitations of the medium on the in-medium interaction, for instance the G-matrix in the Brueckner approach.

In conclusion, our calculation predicts a quenching of the opacity of nuclear matter to the neutrino propagation and then provides the quantitative basis to estimate the energy release in the supernovae explosions and the rapid cooling of a protoneutron star.

- 
- [1] J.M. Lattimer, C.J. Pethick, M. Prakash and P. Haensel, Phys. Rev. Lett. **66**, 2071 (1991).
- [2] E.N.E. Van Dalen, A.E.L. Dieperink, A. Sedrakian and R.G.E. Timmermans, A&A, **360**, 549 (2000).
- [3] N. Iwamoto and C. J. Pethick, Phys. Rev. D **25**, 313 (1982).
- [4] A. Burrows and R. F. Sawyer, Phys. Rev. C **58**, 554 (1998).
- [5] A. Burrows and R. F. Sawyer, Phys. Rev. C **59**, 510 (1999).
- [6] S. Reddy, M. Prakash, and J. M. Lattimer, Phys. Rev. D **58**, 013009 (1998).
- [7] S. Reddy, M. Prakash, J. M. Lattimer, and J.A. Pons, Phys. Rev. C **59**, 2888 (1999).
- [8] J. Margueron, J. Navarro, N. Van Giai and W. Jiang, Neutrino propagation in neutron matter and the nuclear equation of state, *The Nuclear Many-body Problem 2001*, NATO Science Series II (Kluwer Academic Publ.).
- [9] U. Lombardo, C.W. Shen, N. Van Giai and W. Zuo, Nucl. Phys. **A 722**, 532c (2003).
- [10] J. Margueron, I. Vidaña and I. Bombaci, nucl-th/0307073.
- [11] G. Fabri and F. Matera, Phys. Rev. C **54**, 2031 (1996).
- [12] S. Yamada and H. Toki, Phys. Rev C **61**, 015803 (2000).
- [13] L. Mornas and A. Perez, Eur. Phys. J. **A 13**, 383 (2002).
- [14] L.B. Leinson, Nucl. Phys. **A707**, 543 (2002).
- [15] L. Mornas, nucl-th/0210035.
- [16] C.J. Horowitz and M.A. Pérez-García, astro-ph/0305138.
- [17] K. M. Graczyk and J.T. Sobczyk, nucl-th/0303054.
- [18] R. Niembro, P. Bernados, M. Lopez-Quelle and S. Marcos, Phys. Rev. C **64**, 055802 (2001).
- [19] W. Zuo, A. Lejeune, U. Lombardo, J.-F. Mathiot, Nucl. Phys. **A706**, 418 (2002).
- [20] W. Zuo, A. Lejeune, U. Lombardo, J.-F. Mathiot, Eur.Phys. J. **A 14**, 469 (2002).
- [21] H.Q. Song, M. Baldo, G. Giansiracusa and U. Lombardo, Phys. Rev. Lett. **81**, 1584 (1998).
- [22] F. Osterfeld, Rev. Mod. Phys. **64**, 491 (1992).
- [23] T. Suzuki and H. Sakai, Phys. Lett. **B 455**, 25 (1999).
- [24] R.B. Wiringa, V.G.J. Stocks, R. Schiavilla, Phys. Rev. C **51**, 38 (1995).
- [25] P. Grangé, A. Lejeune, M. Martzoff and J.-F. Mathiot, Phys. Rev. C **40**, 1040 (1989).
- [26] S. Fantoni, A. Sarsa and K.E. Schmidt, Phys. Rev. Lett. **87**, 181101 (2001).
- [27] I. Vidaña, A. Polls and A. Ramos, Phys. Rev. C **65**, 035804 (2002).

- [28] W. Zuo, U. Lombardo and C.W. Shen, in *Quark-Gluon Plasma and Heavy Ion Collisions*, edited by W.M. Alberico et al. (World Scientific, Singapore, 2002), p.192.
- [29] I. Vidaña and I. Bombaci, Phys. Rev. C **66**, 045801 (2002).
- [30] W. Zuo, I. Bombaci and U. Lombardo, Phys. Rev. C **60**, 024605 (1999).